Journal of Applied Sciences, Engineering and Technology for Development. Volume 4, Issue 1

Research Article **ISSN 2309-0936**

Maize crop monitoring with sentinel-1 radar satellite- case study of Endebess, Kenya

Kuria, T. B.[a*], Kirimi, K. F.[b], Gikwa, W. C.[a] and Kuria, N. D.[a]

[a]Dedan Kimathi University of Technology, Nyeri, Kenya

[b]*Jomo Kenyatta University of Agriculture and Technology, Juja, Kenya*

[*]P.O BOX 657-10100, Nyeri, Kenya; kuria.thiongo@dkut.ac.ke

Received :November 2019; Revised: May 2020; Accepted: August 2020

Abstract

Monitoring of crop status coupled with knowledge of growth stages of each crop is a requirement for sustainable agriculture management. Monitoring the crop condition manually in the field is labour, cost and time intensive. Remote sensing therefore provides fast, cost effective and timely tools necessary for the effective monitoring of the crops. The acquisition of cloud free optical images in tropical regions remains a big challenge since the cropping season is characterized by high cloud cover. Radar images which are independent of weather conditions were therefore preferred in this study due to their consistent acquisitions. The objective of this study was to analyse the performance of Sentinel-1 (S-1) C-band radar images in monitoring the maize growth by investigating the transferability of the maize phenological characteristics from one season to the other. This was accomplished by comparing the S-1 backscatter values for the 2015 and 2016 cropping seasons. The acquired S-1 images were divided into three, according to the acquisition modes: ascending IW1; descending IW1; descending IW3. 18 ADC Olngatongo Company maize fields were selected, with the principal maize growth and development stages being defined by the BBCH scale. From the results, the maize phenological development stages could be identified from the images. The backscatter values for fields having coincident planting dates for both 2015 and 2016 had higher similarities compared to fields whose planting dates were far apart. The ascending IW1 had the best results. The results were however inconclusive since fewer images were available for 2015 for comparison with 2016. Thus, a comparison across the entire cropping season could not be conclusively undertaken. From the study, it was concluded that the phenological characteristics extracted for one cropping season can establish a baseline for the monitoring of the subsequent cropping seasons, which can be an indicator of expected yields.

Keywords: Radar, Sentinel-1, Maize BBCH, Phenology mapping

DOI: 10.33803/JASETD.2020.4-1.1

1. INTRODUCTION

Agriculture remains the backbone of Kenya's economy, with maize being identified as the country's staple food (Kipkorir et al., 2007). Trans Nzoia county has been identified as the country's food basket, with majority of the farmers relying on rainfall as the source of water for the crops (Kirimi, 2012). However, over the years, this has become unreliable mainly due to the changes in weather patterns (Jones, 2013). The net effect of these weather conditions on the crop growth require to be periodically monitored to avoid great yield losses. One crop monitoring approach has been carrying out of physical field visits spread across the crop growth period (Kihara et al., 2012). These visits have however proven to be ineffective due to the cost factor, coupled with the lack of a monitoring and evaluation process to confirm that the field visits were indeed carried out. An alternative monitoring approach has been through satellite images.

Satellite images supply data continuously with frequent revisit periods, are operationally sustainable, timely and have a wide geographical coverage (Attema et al., 2009) and thus have been applied in the mapping and monitoring of various crops. Satellites with optical and radar sensors have been used for this purpose since the reflectance from the crops' surface can be related to the different crops' structure and their phenological stage (Dusseux et al., 2014; Lussem et al., 2016; Navarro et al., 2016; Sabour et al., 2008). In tropical areas like Kenya however, optical sensors are affected by cloud cover and haze, which are predominant during the cropping season (Castillejo-González et al., 2009; Devadas et al., 2012). Therefore studies have advocated the use of radar sensors as they are independent of weather conditions (Woodhouse, 2006; Mróz & Mleczko, 2008; Sabour et al., 2008; Baghdadi et al., 2009).

Even though radar images are independent of weather conditions, the images cost factor has been a major hinderance in their application especially in third world countries (Vinciková et al., 2010). However, with the advent of the freely available high-resolution Sentinel-1 (S-1) radar images, there has been a paradigm shift in the monitoring of agriculture fields using radar images (Torres et al., 2012). S-1 with a revisit time of 6 days in 1A and 1B constellation, and images with up to 5 meters spatial resolution has been successfully used for crop mapping for food security (Attema et al., 2009; Veloso et al., 2017). With the increased number of acquisitions during the growing season (six-day temporal resolution), proper sampling of the crops' growth cycles even where the sowing dates may be different dates throughout the region is possible (Torres et al., 2012).

The monitoring of the maize crops during the cropping season was done with the Biologische Bundesanstalt, Bundessortenamt und CHemische Industrie (BBCH) scale (Meier et al., 2010). The BBCH scale outlines the main growth/phenological stages of the maize development from germination to senescence, describing in detail the visible physical changes that occur in the maize plant, for example, the number of unfolded leaves or the number of detectable nodes. A unique code is assigned to every one of these phenological stages.

The objective of this study was therefore to apply the S-1 C-band radar images in monitoring the maize growth for the 2015 and 2016 cropping seasons. The transferability of the maize phenological characteristics from one season to the other was also analyzed by comparing the S-1 backscatter values for the 2015 and 2016 cropping seasons. S-1 images were acquired and analyzed for the two seasons. Maize fields were selected from a large-scale maize growing company were identified in

Endebess area, Trans Nzoia county. The company (ADC Olngatongo) maize crop management data was compared to the analyzed S-1 data. The acquired S-1 images were divided into three, according to the acquisition modes: ascending IW1; descending IW1; descending IW3. 18 ADC Olngatongo Company maize fields were selected from the different planting blocks, with the principal maize growth and development stages being defined by the BBCH scale. In the end the transferability of the backscatter characteristics from on cropping season to the next will be analyzed.

2. METHODS

2.1 STUDY AREA

The study area (Figure 1) is located in Endebess, Kenya with center coordinates: latitude 1.067°, longitude 34.867° and an average elevation of 1900 meters above sea level (Dixit et al., 2011). It is classified under the Lower Highland 3 (LH3) agricultural ecological zone with an average annual rainfall of between 970-1300 mm and a mean annual temperature of 18.6°C (Government of Kenya, 2012; Jaetzold & Schmidt, 1982; Ransom et al., 1997). The soil consists of humic and eutric Nitisols that are deep, well drained, fertile soils that are slightly acid to neutral (pH 5.5-7.0) (Gachene & Kimaru, 2004). Due to these conducive climate and soil conditions, the area is characterized by both large scale and small scale agricultural farming activities (Moore et al., 2014). The maize crop is grown either for silage, as seed maize, for commercial or subsistence purposes. The area has two maize cropping seasons, March – September, and October – May (FAO, 2010). The main maize cropping season, however, is March-September during the long rains. The maize fields that were considered for this study had a minimum size of 10 Ha and a maximum size of 40 Ha. The fields were under the management of a well-established company, the Agricultural Development Corporation (ADC) Olngatongo. This was to ensure consistency in the field management procedures.

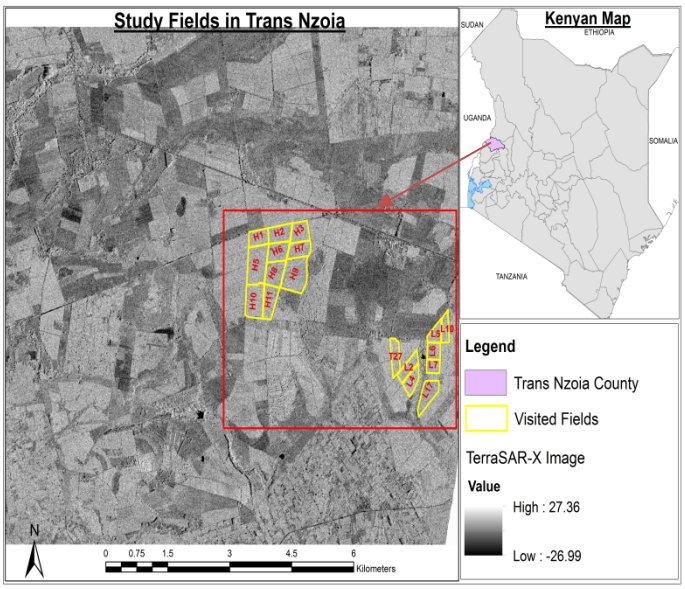

Figure 1. The Endebess study fields in Trans Nzoia County, Kenya.

2.2 SENTINEL-1 IMAGES

The S-1 was launched in 2014 by the European Union and European Space Agency (EU-ESA) within the Copernicus programme that had identified marine core services, land monitoring, and emergency services as some of the priority areas (Malenovský et al., 2012). It is a radar imaging mission at C-band consisting of a two satellites constellation launched in 2014 (S-1A) and 2016 (S-1B) (Attema et al., 2009). It is a near polar sun-synchronous satellite with an altitude of 693 km, a 6-day repeat with an incidence angle of 31°- 46°. It images in four exclusive imaging modes with different resolutions (down to 5 meters) and coverage (up to 400 km). This mission provides dual polarization capability in a single pass (ascending or descending) (Attema et al., 2009).

2.3 FIELD DATA

The image backscatter values are dependent on the phenological stage of the crops and therefore information about the maize crop fields was collected (McNairn et al., 2009). The attribute data that was collected included information about the fields and the crops in them. This included: the official name and sizes of the fields as appearing in the company records; the maize cultivar planted in the field, the planting, emergence, flowering, bulking, physiological maturity and harvesting dates; the BBCH-code related to a particular crop stage; the plant population density; the planting direction; the farm management activities undertaken (fertilizer application, top dressing, weeding); the date of the field visit and any notable remarks.
Similar field management practices were carried out in all the fields since they were under the same maize company. Eighteen maize fields were then randomly selected as the study fields such that the different planting blocks were covered.

2.4 DATA PROCESSING

The S-1 interferometric wide swath (IWS), single look complex (SLC) products were acquired as individual burst images comprising of three single sub-swath datasets, namely IW1, IW2, and IW3, for each polarization acquired. In order to preserve the sensors' original resolution, the S-1 images datasets were processed starting from the SLC format and slant range geometry (Breit et al., 2010; Mittermayer et al., 2010). The steps included: split; de-burst; multi-looking; calibration; terrain correction; speckle filtering; linear to dB conversion. The SNAP 3.0 toolbox was used. Splitting the datasets ensured that each sub-swath was processed individually. Each sub-swath image consists of a series of bursts, where each burst has been processed as a separate SLC image with black-fill demarcation in between. The images for all bursts in all sub-swaths of an IW SLC product were resampled to a common pixel spacing grid in range and azimuth to ensure burst synchronization for IW products while preserving the phase. Since every burst within any single sub-swath was processed as a single image, the de-bursting step resolves the various bursts within any single sub-swath into one image (Torres et al., 2012).

Geometric and radiometric calibration (Figure 2) of the backscatter values were necessary for inter-comparison of radar images acquired with different sensors, or even of images obtained by the same sensor if acquired in different modes or processed with different processors (Baghdadi et al., 2009). The calibration process took care of both radiometric and absolute calibration. Radiometric calibration minimized the incompatibility in images taken under different observation conditions like the incidence angles or the ascending/descending mode by the different radar sensors (Naught & Naught, 2014), absolute calibration allowed taking into account all contributions in the radiometric values that were not due to the target characteristics. This permits to minimize the differences in the image radiometry and to make any images obtained from different incidence angles, ascending-descending geometries and/or opposite look directions easily comparable and even compatible to acquisitions made by other radar sensors. This was done by the computation of Beta Naught and Sigma Naught (infoterra, 2008).

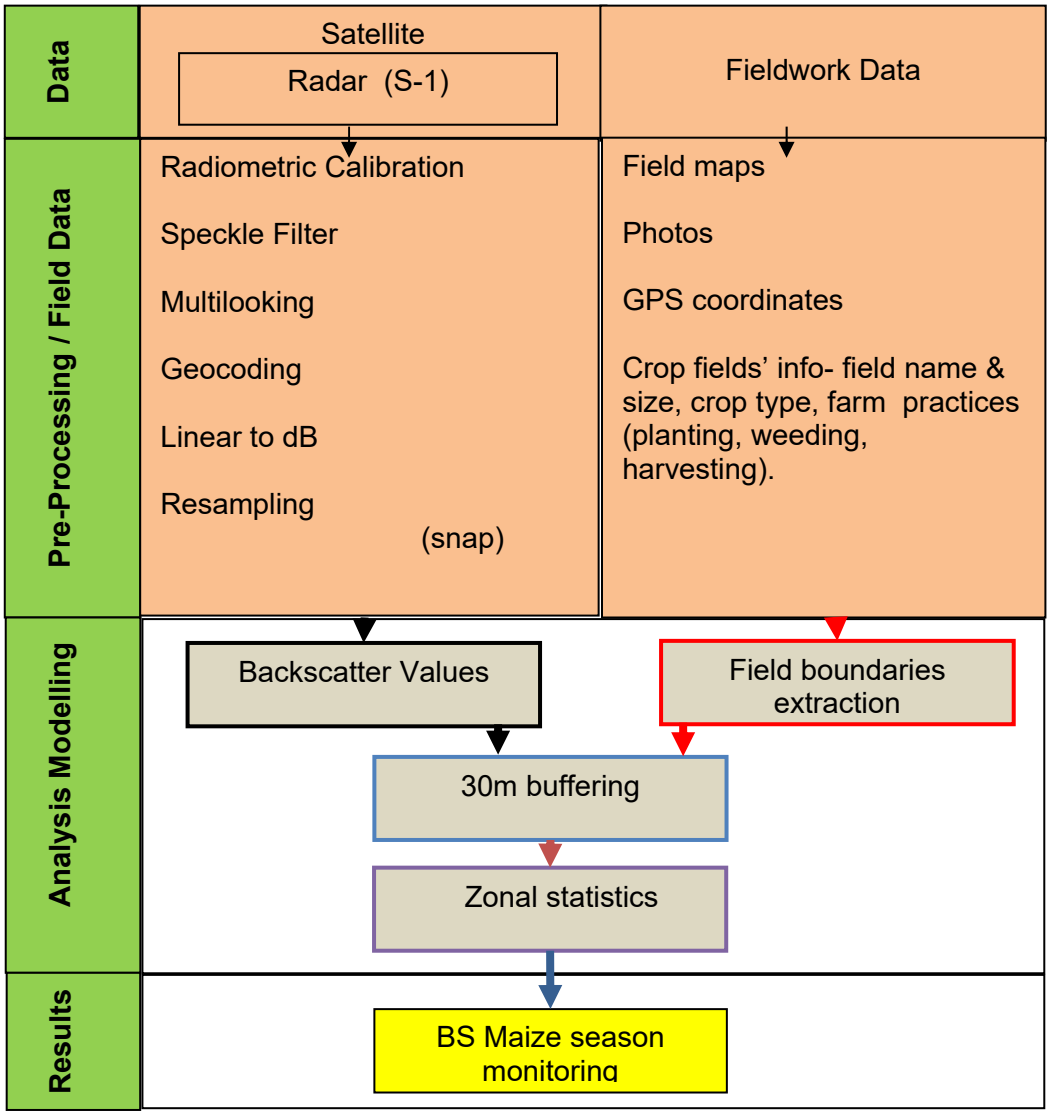

Figure 2. The methodological work flow carried out in the research.

The radar brightness (Beta Naught β^0) representing the radar reflectivity per unit area in slant range was obtained by multiplying the calibration factor with the power of the digital numbers (integer pixel values) using (1). This was then converted into decibel (dB) values using (2).

$$\beta^0 = k_s \bullet \|DN\|^2 \quad (1)$$

$$\beta^0_{db} = 10 \bullet \log_{10}(\beta^0) \quad (2)$$

$$\sigma^0 = \beta^0 \bullet \sin \theta_{loc} \quad (3)$$

Where:

β^0= Beta Naught or radar brightness representing the radar reflectivity per unit area in slant range.

β^0_{db} = Beta Naught in decibels

DN = Digital numbers or image pixel values

σ^0 = Sigma Naught

θ_{loc} = Local incidence angle

k_s = Calibration factor

The local incidence angle (angle between the radar beam and the normal to the illuminated surface) was necessary for the Sigma Naught σ^0 (radar reflectivity per unit area in ground range) calculations. The backscatter from the crop type surfaces was influenced by the relative orientation of the illuminated cell and the sensor and also the distance in range between them (Eineder et al., 2008). Equation (3) was applied.

The speckle effect is a spatially random multiplicative noise due to the coherent superposition of multiple backscatter sources within a SAR resolution element caused by interference of backscattering objects below the geometric resolution within one resolution pixel of the sensor (Lemp & Koch, 2009). Speckle reduction was carried out iteratively with multi-looking using a Lee Sigma filter with a 7x7 window size.

In the terrain correction processing step, the TanDEM-X 12 meter digital elevation model (DEM) was used (Pitz & Miller, 2010). The bilinear interpolation resampling method was applied. The pixels were resampled to 10 meters and the map projection was UTM/WGS 84. The backscatter values were then converted to decibels (dB). All the images were then co-registered, with the S-1 image acquired on the 8/05/2015 being used as the reference image. The image backscatter reflectance values were computed at the fields' level using the zonal statistics tool in ArcGIS 10.3.1. A buffer of 30 meters from each field boundary was used to eliminate the effect of mixed or undesirable field edge pixels in the statistics (Abuzar, 2014).

3. RESULTS AND DISCUSSION

Multiplot graphs of backscatter values against the day of the year were plotted for the 18 maize fields. The multiplots were divided according to the available image acquisition modes: ascending IW1; descending IW1; descending IW3 (Figures 3, 4, and 5). The fields H1-H11 had the same maize variety for both 2015 and 2016 (H6213) whereas fields L2-T27 had the maize variety H628 for 2015, and H614 for 2016. Two sets of vertical lines, one for 2015 and the other for 2016 were utilized to indicate the start and end of the cropping period for the two years.

From (Figure 3) - ascending IW1, some phenological stages for both 2015 and 2016 backscatter values were comparable, despite the differences in the planting period or the maize variety cultivated. For example, H9 and L10. For fields whose planting dates were close for the two years, their backscatter values are comparable (H7, L2, L10). There were also instances where the backscatter values for the two years were still comparable, despite the planting dates being apart (H9, L17). The number of images available played a role in comparing the two image sets. More images were available in 2016 as compared to 2015 and therefore the time epochs within the growing season lacked images for comparison (H7).

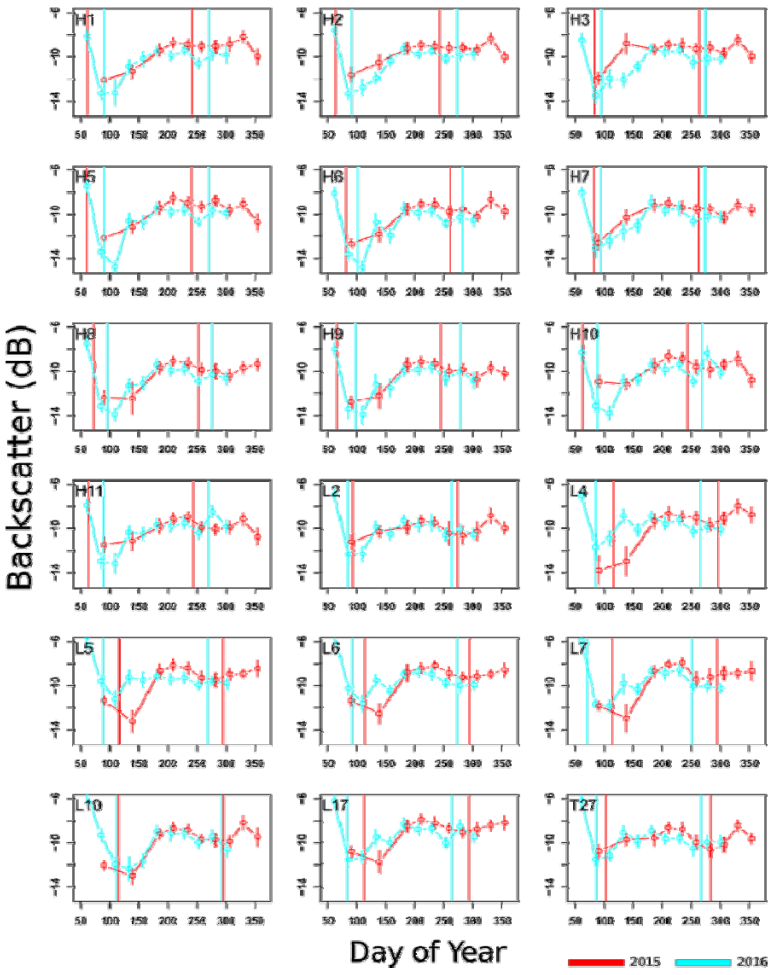

Figure 3: A multiplot of the Sentinel-1 (S-1) ascending IW1 mode backscatter values for the 18 ADC Olngatongo maize fields analyzed for the 2015 and 2016 cropping

seasons. The vertical lines indicate the planting and end of growth period for the maize in the fields.

For the descending IW1 (Figure 4) and the descending IW3 (Figure 5), comparison of the two years was limited by the few available images for 2015. Backscatter values were comparable for epochs where both sets of images were available, though a comparison across the entire cropping season could not be conclusively undertaken.

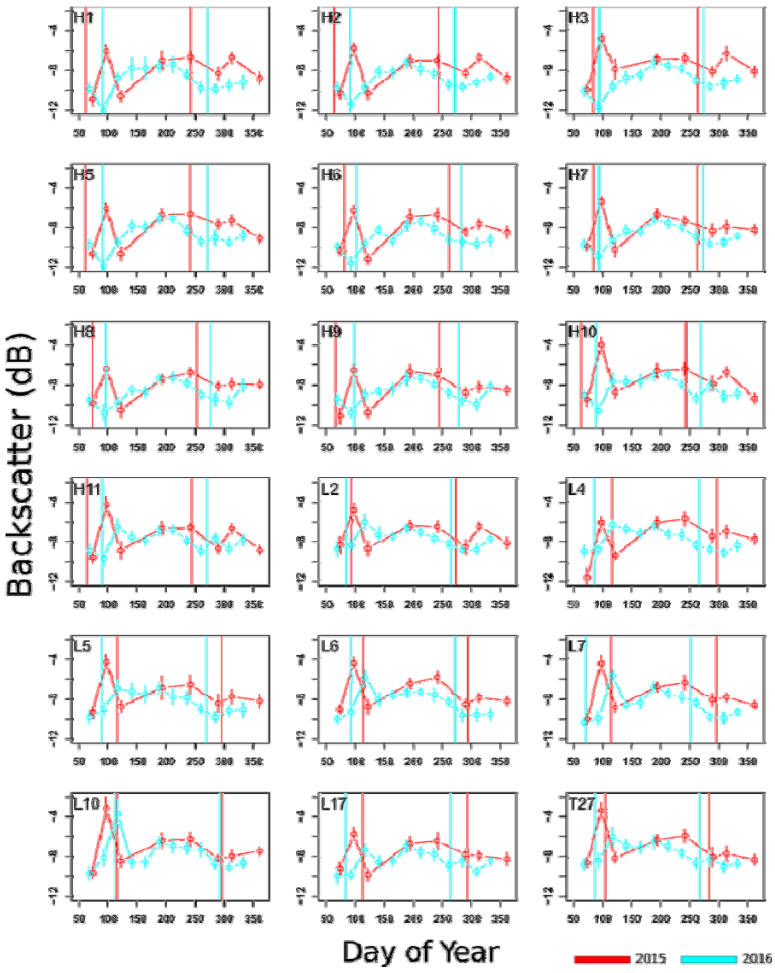

Figure 4: A multiplot of the Sentinel-1 (S-1) descending IW1 mode backscatter values for the 18 ADC Olngatongo maize fields analyzed for the 2015 and 2016 cropping seasons. The vertical lines indicate the planting and end of growth period for the maize in the fields.

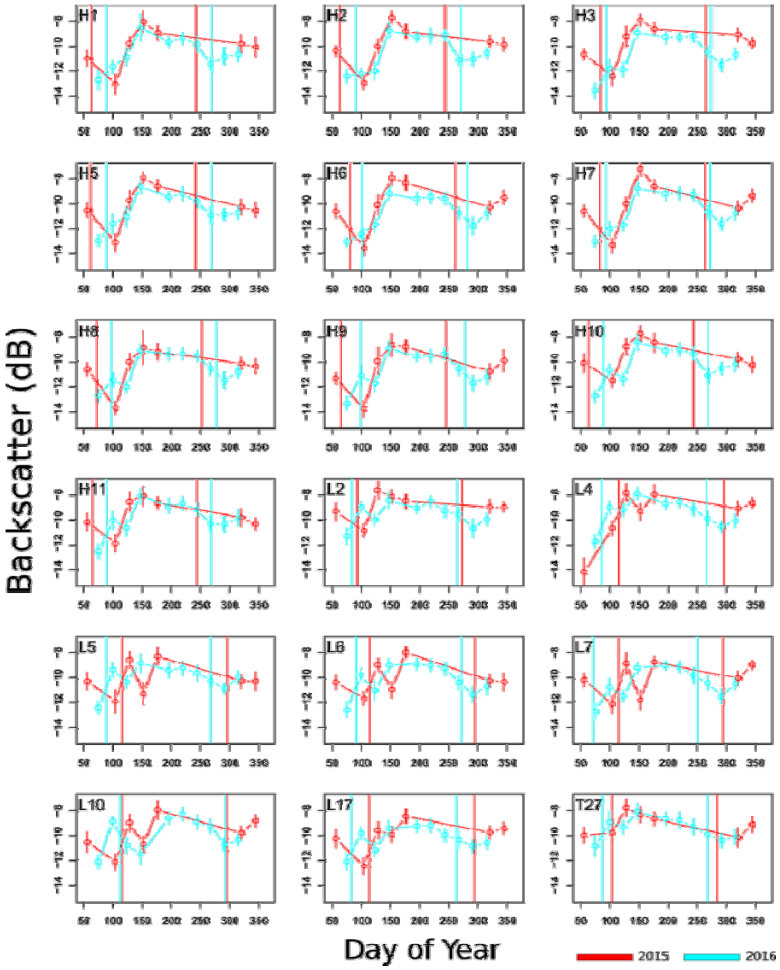

Figure 5: A multiplot of the Sentinel-1 (S-1) descending IW3 mode backscatter values for the 18 ADC Olngatongo maize fields analyzed for the 2015 and 2016 cropping seasons. The vertical lines indicate the planting and end of growth period for the maize in the fields.

4. CONCLUSION

The capability of comparing the maize phenological characteristics from one year to the next with S-1 data was investigated. The images were available in ascending IW1, descending IW1, and descending IW3. From the results (Figures 3, 4, and 5), the VV ascending IW1 mode produced the best results. Notably, this also had the highest number of images for both 2015 and 2016. Thus, the limitation occasioned by the unavailability of adequate S-1 images in 2015 to match the 2016 acquisitions rendered the outcome inconclusive. Comparing the maize varieties cultivated for the two seasons (H6213 for both years; and H628 for 2015 and H614 for 2016), the backscatter values were found to be independent of the maize varieties planted. The backscatter values were rather influenced by the planting dates for the two years. For fields whose planting dates were not far apart, their backscatter values were comparable, compared to fields whose planting dates were far apart. The maize phenological stages could also be detected from the backscatter values for the two years. This was the case for even fields with a difference in the 2015 and 2016 planting dates. As long as the maize crops were at similar phenological development stages for the two years, then their backscatter values were comparable. The backscatter characteristic curve from one year can therefore form a baseline to monitor the condition of maize in the field for the subsequent years.

ACKNOWLEDGEMENT

My appreciation to the Olngatongo Agricultural Development Corporation Kenya (ADC) farm for the ground reference data, the universities of Bonn and Bochum for the technical support, and the Katholische Akademische Ausländer Dienst (KAAD) for the financial support,.

REFERENCES

Abuzar, M. (2014). Comparing Inter-Sensor NDVI for the Analysis of Horticulture Crops in South-Eastern Australia. *American Journal of Remote Sensing*, *2*(1), 1. https://doi.org/10.11648/j.ajrs.20140201.11

Attema, E., Davidson, M., Snoeij, P., Rommen, B., & Floury, N. (2009). Sentinel-1 mission overview (pp. I-36-I–39). IEEE. https://doi.org/10.1109/IGARSS.2009.5416921

Baghdadi, N., Boyer, N., Todoroff, P., El Hajj, M., & Bégué, A. (2009). Potential of SAR sensors TerraSAR-X, ASAR/ENVISAT and PALSAR/ALOS for monitoring sugarcane crops on Reunion Island. *Remote Sensing of Environment*, *113*(8), 1724–1738. https://doi.org/10.1016/j.rse.2009.04.005

Breit, H., Fritz, T., Balss, U., Lachaise, M., Niedermeier, A., & Vonavka, M. (2010). TerraSAR-X SAR Processing and Products. *Institute of Electrical & Electronics Engineers (IEEE)*, *48*(2), 727--740. https://doi.org/10.1109/tgrs.2009.2035497

Castillejo-González, I. L., López-Granados, F., García-Ferrer, A., Peña-Barragán, J. M., Jurado-Expósito, M., de la Orden, M. S., & González-Audicana, M. (2009). Object- and pixel-based analysis for mapping crops and their agro-environmental associated measures using QuickBird imagery. *Computers and Electronics in Agriculture*, *68*(2), 207–215. https://doi.org/10.1016/j.compag.2009.06.004

Devadas, R., Denham, R., & Pringle, M. (2012). Support Vector Machine Classification of Object-based Data for Crop Mapping, Using Multi-temporal Landsat Imagery. *ISPRS Archives*, *39*, B7.

Dixit, P. N., Cooper, P., Dimes, J., & Rao, K. P. (2011). Adding Value to Field-Based Agronomic Research through Climate Risk Assessment: A Case Study of Maize Production in Kitale, Kenya. *Experimental Agriculture*, *47*(02), 317–338. https://doi.org/10.1017/S0014479710000773

Dusseux, P., Corpetti, T., Hubert-Moy, L., & Corgne, S. (2014). Combined Use of Multi-Temporal Optical and Radar Satellite Images for Grassland Monitoring. *Remote Sensing*, *6*(7), 6163–6182. https://doi.org/10.3390/rs6076163

Eineder, M., Fritz, T., Mittermayer, J., Roth, A., Boerner, E., & Breit, H. (2008). *TerraSAR-X Ground Segment, Basic Product Specification Document*. DTIC Document. Retrieved from http://oai.dtic.mil/oai/oai?verb=getRecord&metadataPrefix=html&identifier=ADA515513

FAO. (2010). Crop calendar. Retrieved 12 April 2017, from http://www.fao.org/agriculture/seed/cropcalendar/cropcalendar.do

Gachene, C., & Kimaru, G. (2004). *Soil fertility and land productivity. A guide for extension workers in the eastern Africa region. RELMA Technical Handbook Series 30. Nairobi, Kenya RELMA/Sida*. ISBN 9966-896-66-X, 146+ xiv pp.

Government of Kenya. (2012). Environmental and Social Management Framework for Kenya Agricultural Productivity and Agribusiness Project (KAPAP); and Kenya Adaptation to Climate Change in Arid and Semi-Arid Lands Project (KACCAL).

infoterra. (2008). Radiometric Calibration of TerraSAR-X Data. Retrieved from http://www2.astrium-geo.com/files/pmedia/public/r465_9_tsxx-itd-tn-0049-radiometric_calculations_i3.00.pdf

Jaetzold, R., & Schmidt, H. (1982). *Farm management handbook of Kenya* (Vol. 2).

Jones, J. (2013, July 19). Details on crop information to calibrate crop models for kenya. Retrieved from http://www.yieldgap.org/gygamaps/pdf/Details%20on%20crop%20information%20to%20calibrate%20crop%20models%20for%20Kenya.pdf

Kihara, J., Fatondji, D., Jones, J., Hoogenboom, G., Tabo, R., & Bationo, A. (2012). *Improving Soil Fertility Recommendations in Africa Using the Decision Support System for Agrotechnology Transfer (DSSAT)*. Springer Science & Business Media.

Kipkorir, E. C., Raes, D., Bargerei, R. J., & Mugalavai, E. M. (2007). Evaluation of two risk assessment methods for sowing maize in Kenya. *Agricultural and Forest Meteorology*, *144*(3–4), 193–199. https://doi.org/10.1016/j.agrformet.2007.02.008

Kirimi, L. (2012). History of Kenyan maize production, marketing and policies. *Tegemeo Institute of Agricultural Policy and Development. Nairobi, Kenya*.

Lemp, D., & Koch, B. (2009). Forest monitoring using TerraSAR-X data—evaluation of processing methods and first results. In *Proceedings of TerraSAR-X science meeting*. Retrieved from http://terrasar-x.dlr.de/papers_sci_meet_3/poster/MTH0384_lemp.pdf

Lussem, U., Hütt, C., & Waldhoff, G. (2016). Combined Analysis of Sentinel-1 and RapidEye Data for Improved Crop Type Classification: An Early Season Appraoch for Rapseed and Cereals. *ISPRS - International Archives of the Photogrammetry, Remote Sensing and Spatial Information Sciences*, *XLI-B8*, 959–963. https://doi.org/10.5194/isprsarchives-XLI-B8-959-2016

Malenovský, Z., Rott, H., Cihlar, J., Schaepman, M. E., García-Santos, G., Fernandes, R., & Berger, M. (2012). Sentinels for science: Potential of Sentinel-1, -2, and

-3 missions for scientific observations of ocean, cryosphere, and land. *Remote Sensing of Environment*, *120*, 91–101. https://doi.org/10.1016/j.rse.2011.09.026

McNairn, H., Champagne, C., Shang, J., Holmstrom, D., & Reichert, G. (2009). Integration of optical and Synthetic Aperture Radar (SAR) imagery for delivering operational annual crop inventories. *ISPRS Journal of Photogrammetry and Remote Sensing*, *64*(5), 434–449. https://doi.org/10.1016/j.isprsjprs.2008.07.006

Meier, U., Bleiholder, H., Buhr, L., Feller, C., Hack, H., Hess, M., … others. (2010). Das BBCH-System zur Codierung der phänologischen Entwicklungsstadien von Pflanzen–Geschichte und Veröffentlichungen. *Journal Für Kulturpflanzen*, *61*(2), 41–52.

Mittermayer, J., Prats, P., Piantanida, R., Sauer, S., Guarnieri, A. M., Attema, E., … others. (2010). TOPS Sentinel-1 and TerraSAR-X processor comparison based on simulated data. In *Synthetic Aperture Radar (EUSAR), 2010 8th European Conference on* (pp. 1–4). VDE. Retrieved from http://ieeexplore.ieee.org/xpls/abs_all.jsp?arnumber=5758741

Moore, N., Serafin, L., & Jenkins, L. (2014). Summer crop production guide 2 0 14. NSW Department of Primary Industries. Retrieved from http://www.dpi.nsw.gov.au/__data/assets/pdf_file/0005/303485/Summer-crop-production-guide-2014.pdf

Mróz, M., & Mleczko, M. (2008). Potential of Terrasar-X stripmap data in early and rapid agricultural crops mapping. In *TerraSAR-X Science Team Meeting, DLR–Oberpfaffenhofen, Germany*. Retrieved from http://phoenix.caf.dlr.de/papers_sci_meet_3/paper/LAN0167_mroz.pdf

Naught, B., & Naught, S. (2014). Radiometric Calibration of TerraSAR-X Data.

Navarro, A., Rolim, J., Miguel, I., Catalão, J., Silva, J., Painho, M., & Vekerdy, Z. (2016). Crop Monitoring Based on SPOT-5 Take-5 and Sentinel-1A Data for the Estimation of Crop Water Requirements. *Remote Sensing*, *8*(6), 525. https://doi.org/10.3390/rs8060525

Pitz, W., & Miller, D. (2010). The TerraSAR-X Satellite. *IEEE Transactions on Geoscience and Remote Sensing*, *48*(2), 615–622. https://doi.org/10.1109/TGRS.2009.2037432

Ransom, J., Palmer, A., Zambezi, B., Mduruma, Z., Waddington, S., Pixley, K., & Jewell, D. (1997). *Maize productivity gains through research and technology dissemination*. CIMMYT.

Sabour, S. T., Lohmann, P., & Soergel, U. (2008). Monitoring Agricultural Activities Using Multi-Temporal ASAR ENVISAT Data. *The International Archives of the Photogrammetry, Remote Sensing and Spatial Information Sciences*, *37*, 735–742.

Torres, R., Snoeij, P., Geudtner, D., Bibby, D., Davidson, M., Attema, E., … Rostan, F. (2012). GMES Sentinel-1 mission. *Remote Sensing of Environment*, *120*, 9–24. https://doi.org/10.1016/j.rse.2011.05.028

Veloso, A., Mermoz, S., Bouvet, A., Le Toan, T., Planells, M., Dejoux, J.-F., & Ceschia, E. (2017). Understanding the temporal behavior of crops using Sentinel-1 and Sentinel-2-like data for agricultural applications. *Remote Sensing of Environment*, *199*, 415–426. https://doi.org/10.1016/j.rse.2017.07.015

Vinciková, H., Hais, M., Brom, J., Procházka, J., & Pecharová, E. (2010). Use of remote sensing methods in studying agricultural landscapes–. *Journal of Landscape Studies*, *3*, 53–63.

Woodhouse, H. I. (2006). *Introduction to Microwave Remote Sensing*. CRC Press.